Electrochimica Acta 200 (2016) 142–151

Contents lists available at ScienceDirect

Electrochimica Acta

journal homepage: www.elsevier.com/locate/electacta

Three-dimensional-networked Ni-Co-Se nanosheet/nanowire arrays on carbon cloth: A flexible electrode for efficient hydrogen evolution

Zhen Zhang[a,b], Yundan Liu[a,b], Long Ren[a,b,d], Han Zhang[c,*], Zongyu Huang[a,b,c], Xiang Qi[a,b,c,*], Xiaolin Wei[a,b], Jianxin Zhong[a,b]

[a] Hunan Key Laboratory of Micro-Nano Energy Materials and Devices, Xiangtan University, Hunan 411105, PR China
[b] Laboratory for Quantum Engineering and Micro-Nano Energy Technology and School of Physics and Optoelectronics, Xiangtan University, Hunan 411105, PR China
[c] Key Laboratory of Optoelectronic Devices and Systems of Ministry of Education and Guangdong Province, Shenzhen University, 518060, PR China
[d] Institute for Superconducting and Electronic Materials, Australian Institute for Innovative Materials, University of Wollongong, Innovation Campus, North Wollongong, New South Wales 2500, Australia

ARTICLE INFO

Article history:
Received 19 February 2016
Received in revised form 29 March 2016
Accepted 30 March 2016
Available online 1 April 2016

Keywords:
$NiSe_2$
$CoSe_2$
anion exchange reaction
hydrogen evolution reaction
electrocatalysis

ABSTRACT

Transition metal diselenides have been considered as one of the most promising earth-abundant electrocatalysts as alternatives to noble metal for the hydrogen evolution reaction (HER). Here, hierarchically three-dimensional nickel cobalt diselenides ($Ni_{1/3}Co_{2/3}Se_2$) with networked nanowires and nanosheets characteristics have been successfully synthesized. Such morphological features may not only provide large surface area allowing for exposure of more active sites, but also benefit deep electrolyte penetration for electrons and electrolyte ions. The resulting binder-free flexible electrodes with large production yield exhibit superior electrochemical HER activity and excellent durability after potential sweep tests for 1000 cycles. Besides their catalytic activity remain stable for electrolysis over 8 h at mixed overpotential. The outstanding electrocatalytic performance makes the present nickel cobalt diselenide as a promising earth-abundant electrocatalyst for HER application.

1. Introduction

Owing to the virtues of high energy density and zero environmental impact of the combustion product, hydrogen is generally considered as a promising alternative and renewable energy source to replace fossil fuels in the future [1–4]. One of the main methods to produce highly pure hydrogen is the electrochemical water splitting, in which the catalysts are usually based on noble metals like platinum (Pt) and their alloys [5–7]. Although Pt-group metals exhibit superior catalytic activity, the high cost and rareness have hampered their widespread application for hydrogen evolution reaction (HER) [8,9]. Therefore, it is still very attractive to develop and design novel high-performance HER catalysts based on active materials that are abundant on earth. Recently, various new HER catalysts are reported, such as transition metal dichalcogenides (MX_2, X = S, Se) including MoS_2 [10], WS_2 [11], $MoSe_2$ [12], WSe_2 [13], metal carbides (Mo_2C [14], WC [15]), metal phosohides (Ni_2P [16], Co_2P [17] and MoP [18]), metal boride (MoB [19]) and metal nitrides (TiN [20]). However, most of them still suffer from the low intrinsic activity and relatively poor electrochemical stability compared with Pt-based materials.

Due to the earth abundance and detailed theoretical analyses of nickel element, a multitude of nickel-based materials have emerged as most promising catalyst for HER [21,22]. It is worth noting that although Ni-based materials are usually capable of efficient HER power, they also suffer from poor stability in acidic solutions because of corrosion issue [23]. According to previous reports, the stability of Ni-based materials can be enhanced by synergistically incorporating other functional materials [24]. For example, Sun et al. reported the preparation of Ni_xS_y-MoS_2 hybrid microspheres by one-pot hydrothermal route. The resulting composite exhibits superior HER catalytic activity and stability over sole MoS_2 and Ni_xS_y [25]. As one of typical non-noble metal chalcogenides, $CoSe_2$ has displayed a particular advantage as electrocatalysts for hydrogen evolution, and various efforts have

* Corresponding authors at: Key Laboratory of Optoelectronic Devices and Systems of Ministry of Education and Guangdong Province, Shenzhen University, 518060, PR China.
E-mail addresses: hzhang@szu.edu.cn (H. Zhang), xqi@xtu.edu.cn (X. Qi).

http://dx.doi.org/10.1016/j.electacta.2016.03.186
0013-4686/

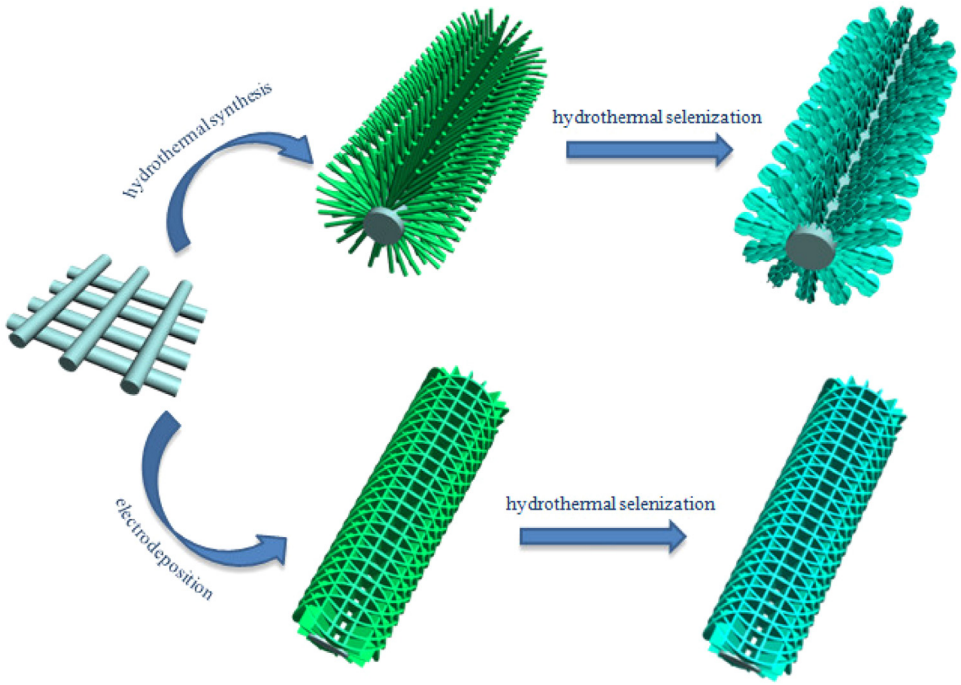

Fig 1. Schematic illustration of the formation mechanism of $Ni_{1/3}Co_{2/3}Se_2$ nanowires and nanosheets grown on carbon cloth.

been devoted to synthesis $CoSe_2$ resultant hybrid materials to achieve excellent catalytic performance with enhanced activity and stability [26]. For example, Yu et al. reported the preparation of $CoSe_2$/DETA (DETA = diethylenetriamine) which showed high catalytic properties for both HER and OER [27,28]. Recently, Zheng group found that the hybrid $CoSe_2/MoS_2$ materials exhibited greatly improved activity and stability than that of pure $CoSe_2$, mainly due to the strong synergistic effect and increased active sites [29]. All above mentioned research inspires us that functionalizing $CoSe_2$ with Ni species could be one possible method to boost their catalytic behavior. Xu et al. reported the preparation of $CoSe_2$ nanobelts decorated by Ni/NiO nanoparticles via a simple solvothermal method and a subsequent annealing process, which reveals enhanced electrochemical HER catalytic performance [30]. Cui et al. successfully converted e-beam evaporated cobalt/nickel double-layer thin-films into ternary nickel cobalt diselenides film using the selenization reaction in a horizontal tube furnace [31]. However, it is still highly necessary and imperative to develop a simple and cost-effectively preparation strategy toward the fabrication of economically ternary nickel cobalt diselenides with large production yield and expected HER catalytic performance.

Generally, in order to further enhance electrochemical HER performance, one of the most effective method is to fabricate and design nanostructured electrocatalysts, which may not only facilitate efficient diffusion of the electrolyte, but also provide enough active sites [32]. Besides, the conductivity of the electrode is also a key factor towards HER. Further enhanced catalytic performance can be achieved by directly growing nanostructured active materials on a conductive 3D substrate such as carbon cloth (CC) to produce binder-free flexible electrodes for HER. The resulting flexible 3D electrodes can not only provide excellent mechanical strength and avoid the use of polymer binders, leading to good mechanical adhesion and improved electrical conductivity, but also effectively increase the catalyst loading and the utilization of catalytic sites [32–34]. Therefore, fabrication of advanced 3D electrodes and optimization of the morphological design are crucial to improve the catalytic performance of catalysts for HER.

In this paper, we describe a facile two-step approach to fabricate nickel cobalt diselenide nanowires and nanosheets on carbon cloth ($Ni_{1/3}Co_{2/3}Se_2$ nanowires/CC and $Ni_{1/3}Co_{2/3}Se_2$ nanosheets/CC): a first low-temperature hydrothermal synthesis of Ni-Co precursor nanowires and electrodeposition of Ni-Co precursor nanosheets respectively on CC followed by hydrothermal

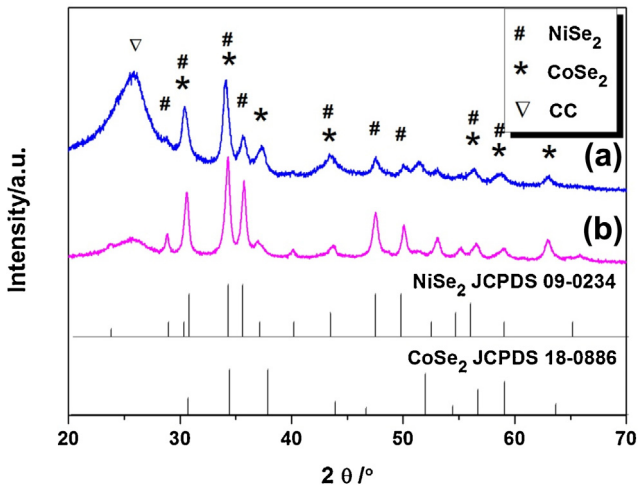

Fig. 2. XRD patterns of $Ni_{1/3}Co_{2/3}Se_2$ nanowires (a) and nanosheets (b).

conversion into $Ni_{1/3}Co_{2/3}Se_2$ via an anion-exchange process (detailed preparation procedure in Supporting Information). The resulting 3D binder-free flexible HER electrodes composed of $Ni_{1/3}Co_{2/3}Se_2$ nanowires or nanosheets show expected high HER performance, with Tafel slop of 40.1 $mVdec^{-1}$ and 46.3 $mVdec^{-1}$, respectively, as well as excellent durability after potential sweeps for 1000 cycles, also maintaining its catalytic activity without distinct loss for at least 8 h. Both the facile preparation and excellent HER behavior have guaranteed the potential application of the obtained 3D binder-free catalytic electrodes toward large-scale hydrogen production from water.

2. Results and discussion

2.1. Structural and morphological characterization

The synthesis of $Ni_{1/3}Co_{2/3}Se_2$ nanowires and nanosheets on CC can be divided into two steps: (1) low-temperature hydrothermal synthesis and electrodeposition of $NiCo_2O_4$ nanowires and nanosheets respectively; (2) conversion of $NiCo_2O_4$ to $Ni_{1/3}Co_{2/3}Se_2$ by the ion-exchange reaction under hydrothermal treatment (Fig. 1). To determine the phase structures of the products, the X-ray diffraction (XRD) measurements are carried out. The XRD results (Fig. S1) of $NiCo_2O_4$ nanowires and nanosheets display a number of peaks at 2θ=18.9°, 31.1°, 36.6°, 44.6°, 59.0° and 64.9°, respectively corresponding to (111), (220), (311), (400), (511) and (440) facets of $NiCo_2O_4$, which perfectly match the standard PDF card JCPDS no. 20-0781 [35]. The broad diffraction peak located at around 2θ=26.3° corresponds to the carbon cloth substrate [36]. Fig. 2 shows the XRD patterns of $Ni_{1/3}Co_{2/3}Se_2$ nanowires (a) and nanosheets (b) on CC substrate. Apparently, the resulting $Ni_{1/3}Co_{2/3}Se_2$ nanowires and nanosheets are mainly composed of $NiSe_2$ (JCPDS card no: 18-0886) [37] and $CoSe_2$ (JCPDS card no: 09-0234) [38], presenting several similar diffraction angles at around 2θ=30.4°, 33.9°, 43.2°, 56.4°, 58.8°, the location of which are extremely close. Except above bands, the peaks positioned at 2θ=28.5°, 35.3°, 47.1°, 49.5° are observed corresponding to (011), (120), (211) and (130) crystal planes of $NiSe_2$, as well as additional peaks at 2θ=37.6°, 63.4°

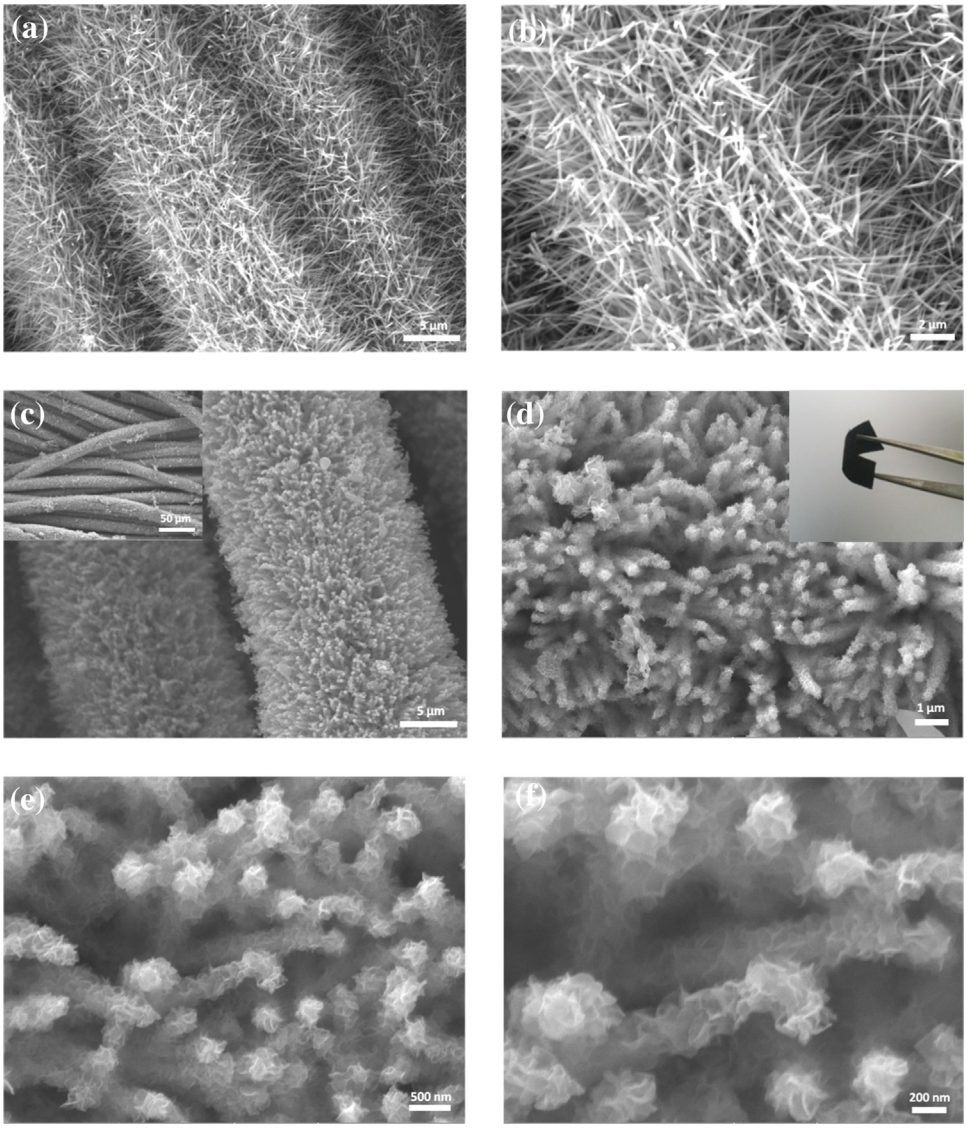

Fig. 3. SEM images for $NiCo_2O_4$ nanowires (a, b), and $Ni_{1/3}Co_{2/3}Se_2$ nanowires (c-f). The inset of (d) is a typical photograph of the flexible electrode.

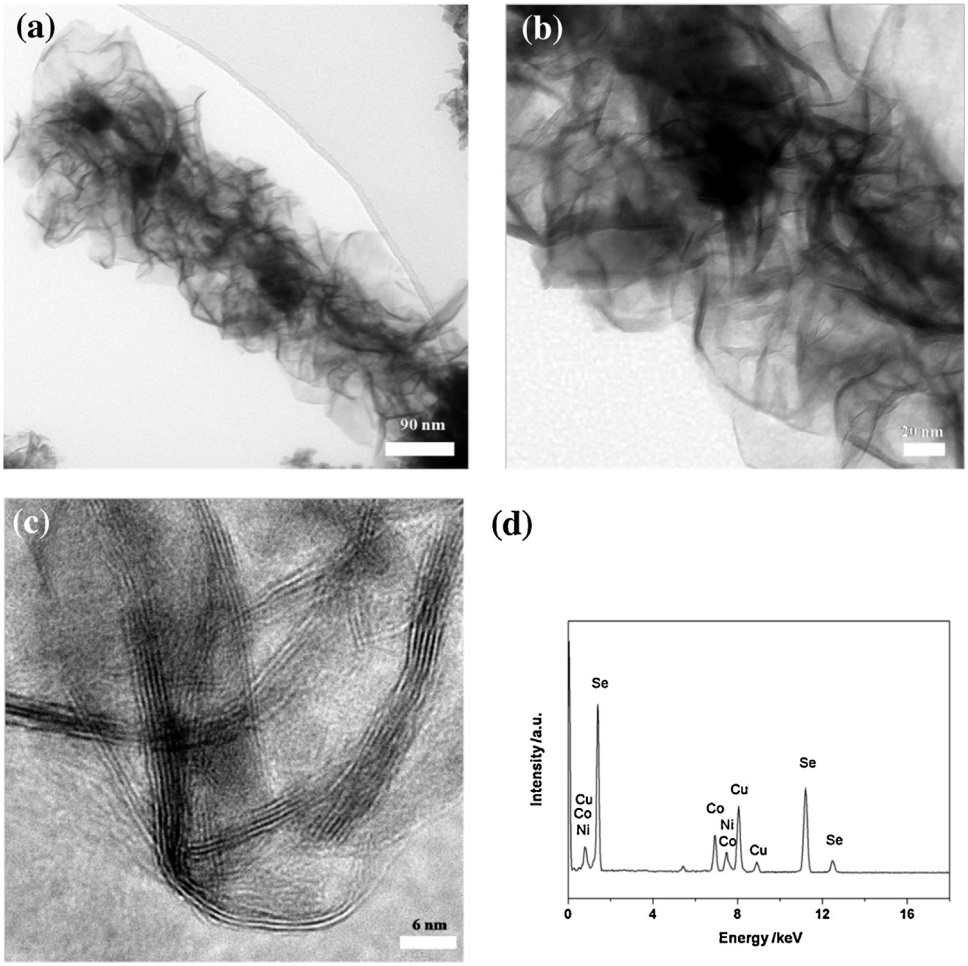

Fig. 4. TEM images (a-c) and EDS spectrum (d) of $Ni_{1/3}Co_{2/3}Se_2$ nanowires.

attributed to (211) and (400) facets of $CoSe_2$, suggesting the successful conversion of $NiCo_2O_4$ to the composite of $NiSe_2$ and $CoSe_2$, which can be approximately labeled as $Ni_{1/3}Co_{2/3}Se_2$. To further confirm the formation of the samples, Raman tests are performed. In Fig. S2, both $Ni_{1/3}Co_{2/3}Se_2$ nanowires and nanosheets exhibit the characteristic peak at around 179 cm^{-1} attributed to the phase of $CoSe_2$ [39], as well as the other one located at 224 cm^{-1} corresponding to bending mode of $NiSe_2$ [40,41]. Above results demonstrate that the $NiSe_2$ and $CoSe_2$ are of co-existence to form ternary diselenides.

SEM images of pure carbon cloth substrate are shown in Fig. S3, which is woven by carbon microfiber with clean and smooth surface. Fig. 3(a,b) shows the $NiCo_2O_4$ nanowire arrays aligned on carbon cloth fabricated by a facile modified hydrothermal process. It is observed that $NiCo_2O_4$ nanowires exhibit sharp tips and their length can reach approximately 4 μm. The final products with high density and yield are distributed on the surface of conductive substrate to form a binder-free electrode. As illustrated by SEM images (Fig. 3(c-f)), after hydrothermal selenization reaction, the $Ni_{1/3}Co_{2/3}Se_2$ product still maintains the 3D integration feature composed of well-aligned nanowire arrays, suggesting the strong adhesion to CC substrate, which is proposed to be beneficial to the outstanding durability performance. Notably, the length of nanowires turns shorten and the sharp tips disappear, and meanwhile the diameter becomes lager. It is worth noting that according to the higher magnification SEM images $Ni_{1/3}Co_{2/3}Se_2$ nanowires with a diameter of approximate 150 nm are characteristically composed of flaky stacks of nanosheets, which is further investigated by Transmission Electron Microscopy (TEM) in Fig. 4(a, b). HRTEM image (Fig. 4c) shows that some of the nanosheets have several folded edges that present different layers of $Ni_{1/3}Co_{2/3}Se_2$ sheets with interlayer spacing of average 0.64 nm. The corresponding selected area electron diffraction (SAED) in Fig. S4a indicates the polycrystalline nature, which is consistent with the XRD results. As demonstrated by the EDS image of the product (Fig. 4d), Ni, Co, and Se elements are coexistent, as well as the Cu element originated from the copper substrate. Fig. 5(a,b) displays the SEM images of $NiCo_2O_4$ nanosheets with different magnifications. Via the electrodepostion process, the surface of carbon cloth is covered with plenty of ordered nanosheets. After the ion-exchange process, $Ni_{1/3}Co_{2/3}Se_2$ nanosheets are obtained, which is shown in Fig. 5(c-f). Each carbon fiber are still uniformly covered by nanosheets, which are interconnected with each other to form a wall-like structure, revealing a 3D hierarchically networked feature with enormous empty space among the adjacent nanosheets. From TEM images (Fig. 6(a,b)), $Ni_{1/3}Co_{2/3}Se_2$ nanosheets are stacked randomly to form the connected

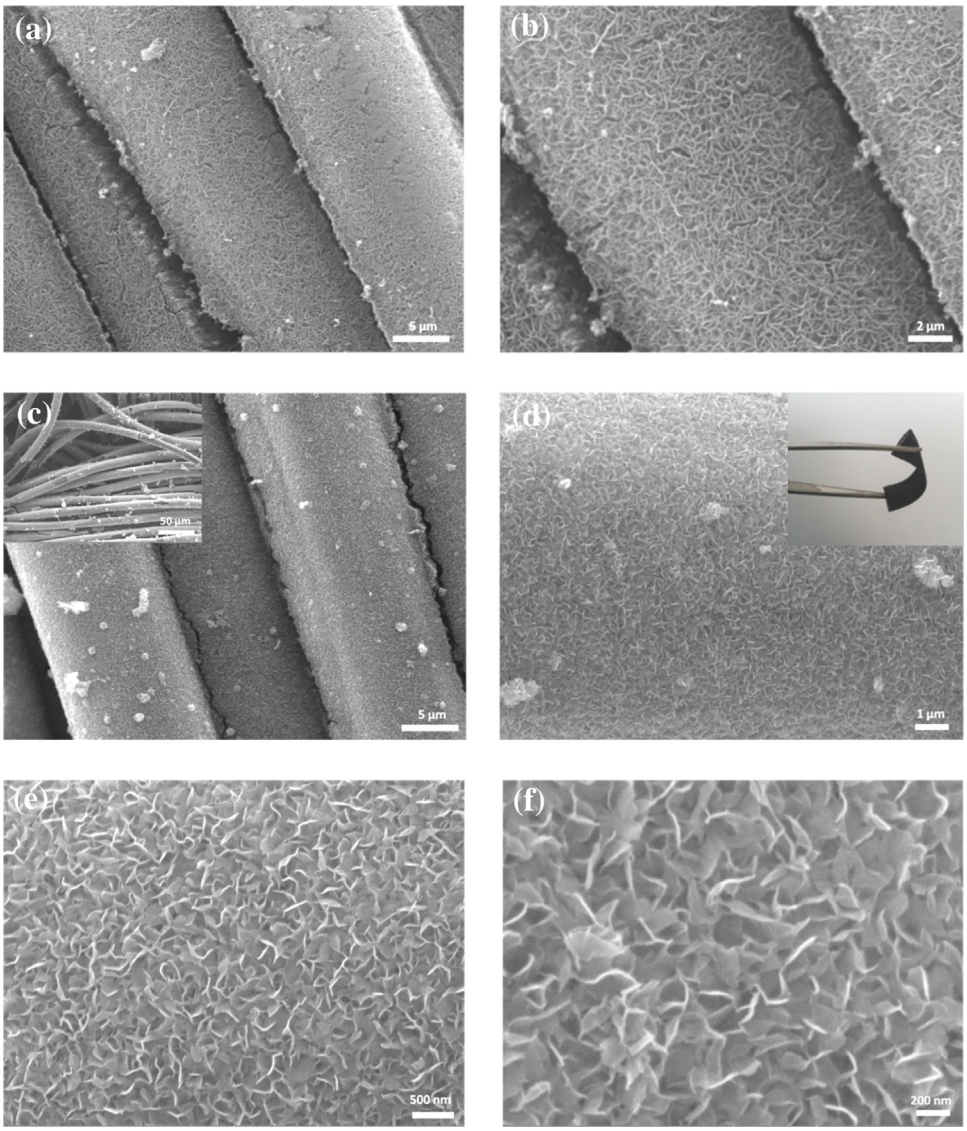

Fig. 5. SEM images for $NiCo_2O_4$ nanosheets (a, b), and $Ni_{1/3}Co_{2/3}Se_2$ nanosheets (c-f). The inset of (d) is shows the flexibility of the electrode.

nanosheet structure and plenty of fold edges are also observed in HRTEM (Fig. 6(c)). The SAED pattern of $Ni_{1/3}Co_{2/3}Se_2$ nanosheets in Fig. S4b is composed of not only bright dots but also rings. Similarly, Ni, Co and Se elements are all observed in the EDS image (Fig. 6d). Therefore, we can draw a conclusion that after the ion-exchange treatment, the 3D nanowires and nanosheets structure characteristics maintain well, but the $Ni_{1/3}Co_{2/3}Se_2$ nanowires are composed of enormous corrugated nanosheets.

XPS measurements are performed to further investigate the chemical bonding state and composition of the as-synthesized $Ni_{1/3}Co_{2/3}Se_2$ nanowires and nanosheets. All of the binding energies obtained in the XPS analysis are corrected for specimen charging by referencing the C 1s peak to 284.6 eV. Fig. 7a displays a high-resolution XPS spectrum of Ni 2p, where two weak peaks centered at 853.6 eV and 869.8 eV can be ascribed to Ni $2p_{3/2}$ and Ni $2p_{1/2}$ orbits, respectively [42]. The Co 2p core level spectrum shows two main peaks with binding energy peaks located at 778.4 and 793.3 eV belonging to Co $2p_{3/2}$ and Co $2p_{1/2}$ respectively, suggesting the existent of Co^{2+} in $CoSe_2$ (Fig. 7b) [32,33]. Fig. 7c reveals two distinct binding energies of 54.8 and 55.7 eV, respectively, which are in good coincidence with the reported data of Se $3d_{5/2}$ and Se $3d_{3/2}$ [43]. As indicated by the survey spectra of the obtained products in Fig. 7d, after the ion-exchange process under hydrothermal treatment, the $NiCo_2O_4$ precursors are successfully converted to ternary nickel and cobalt diselenides.

2.2. HER activity of catalysts

Commercial Pt/C with high HER activity is chosen as a reference point and the bare carbon cloth substrate is also examined for comparison purpose. In order to reflect the intrinsic electrochemical HER activity, an *iR* correction is applied to the whole initial data for further analysis [33]. Fig. 8a exhibits the measured polarization curves of $Ni_{1/3}Co_{2/3}Se_2$ nanowires and nanosheets, bare CC and commercial Pt/C electrode. Clearly, the Pt/C electrode shows the

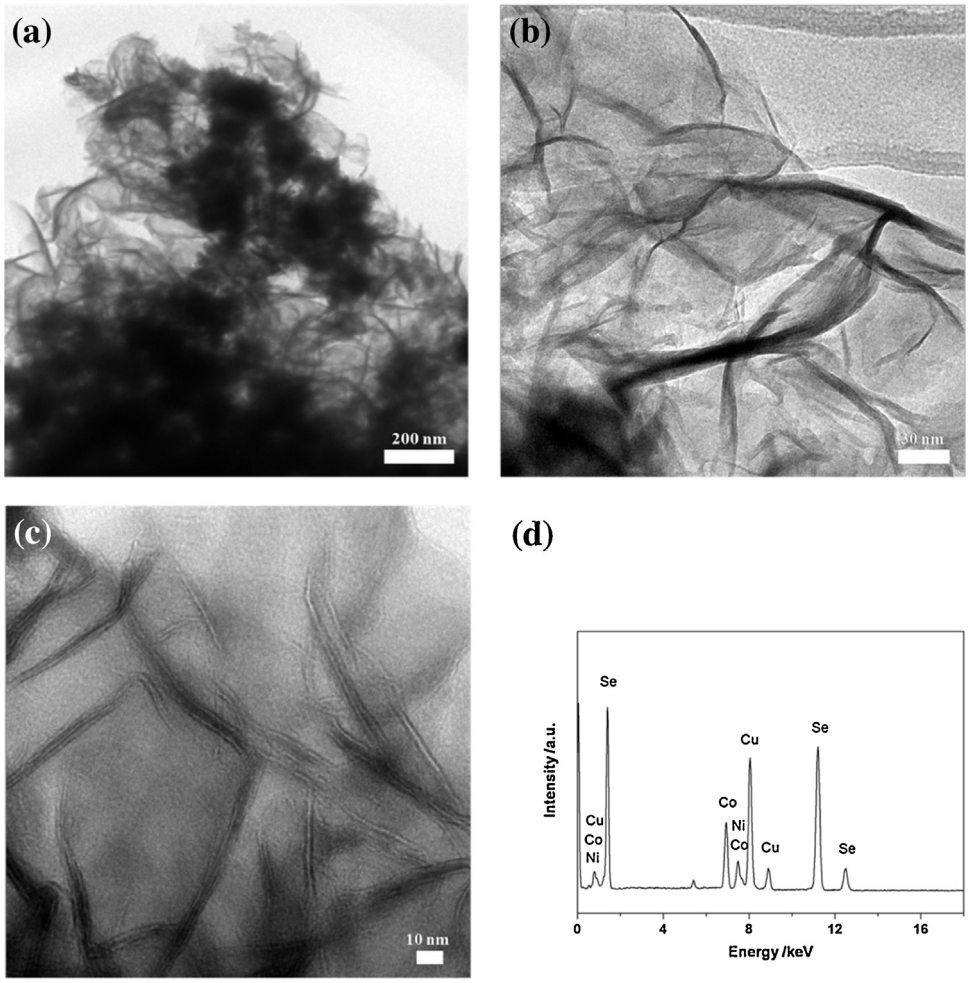

Fig. 6. TEM images (a-c) and EDS spectrum (d) of $Ni_{1/3}Co_{2/3}Se_2$ nanosheets.

best HER properties with near-zero overpotential, whereas bare CC presents poor activity of HER with negligible current flow, suggesting that the HER activities of $Ni_{1/3}Co_{2/3}Se_2$ nanowires and nanosheets 3D electrodes are all contributed to the coating active material on CC substrate. To drive the current density of 0.01 Acm^{-2}, the $Ni_{1/3}Co_{2/3}Se_2$ nanowires and nanosheets require the overpotential of 131 mV_{RHE} and 145 mV_{RHE}, respectively, which are lower than that of some previous reports listed in Table S1 in supporting information. Besides, Tafel slope is another key parameter to evaluate the electrochemical HER activity and a smaller Tafel slope indicates enhanced HER rate at a moderate increase of overpotential. The corresponding Tafel slopes of $Ni_{1/3}Co_{2/3}Se_2$ nanowires, nanosheets and commercial Pt/C electrode are provided in Fig. 8b. Compared with a very small Tafel slope of 30 $mVdec^{-1}$ for Pt/C, the $Ni_{1/3}Co_{2/3}Se_2$ nanowires electrode reveals a Tafel slopes of 40.1 $mVdec^{-1}$, which is slightly smaller than that of $Ni_{1/3}Co_{2/3}Se_2$ nanosheets (46.3 $mVdec^{-1}$), as well as the data reported in some works listed in Table S1, suggesting its great promise for practical hydrogen generation applications. The electrocatalytic parameters of different Ni-Co-Se samples including exchange current density obtained by an extrapolation method is also provided in Table S2.

Stability is another key parameter for hydrogen evolution application. In order to evaluate the durability of the products, stability test is conducted by continuous cyclic voltammetry with the potential range of 200 to −400 mV (vs RHE) for 1000 cycles at an accelerated scanning rate of 100 mVs^{-1}. The polarization curves before and after 1000 cycles are provided in Fig. 8c. More delightfully, it is evident that the cathodic current densities of both $Ni_{1/3}Co_{2/3}Se_2$ nanowires and nanosheets electrodes deliver no distinct loss after cycling test. The morphologies of $Ni_{1/3}Co_{2/3}Se_2$ nanowires and nanosheets after stability test are also examined and provided in Fig. S5, in which the hierarchical nanowire and nanosheet arrays feature retain well, implying the good adhesion between active materials and carbon cloth. Furthermore, the durability of electrocatalysts is also evaluated by electrolysis at a fixed overpotential to drive an initial current density of 0.025 Acm^{-2} for 8 h. Clearly, nearly no loss for the current density of both $Ni_{1/3}Co_{2/3}Se_2$ nanowires and nanosheets is observed in Fig. 8d, demonstrating the excepted catalytic durability.

In order to further understand the electrochemical properties of the $Ni_{1/3}Co_{2/3}Se_2$ nanowires and nanosheets electrodes/solution interfaces, electrochemical impedance spectroscopy

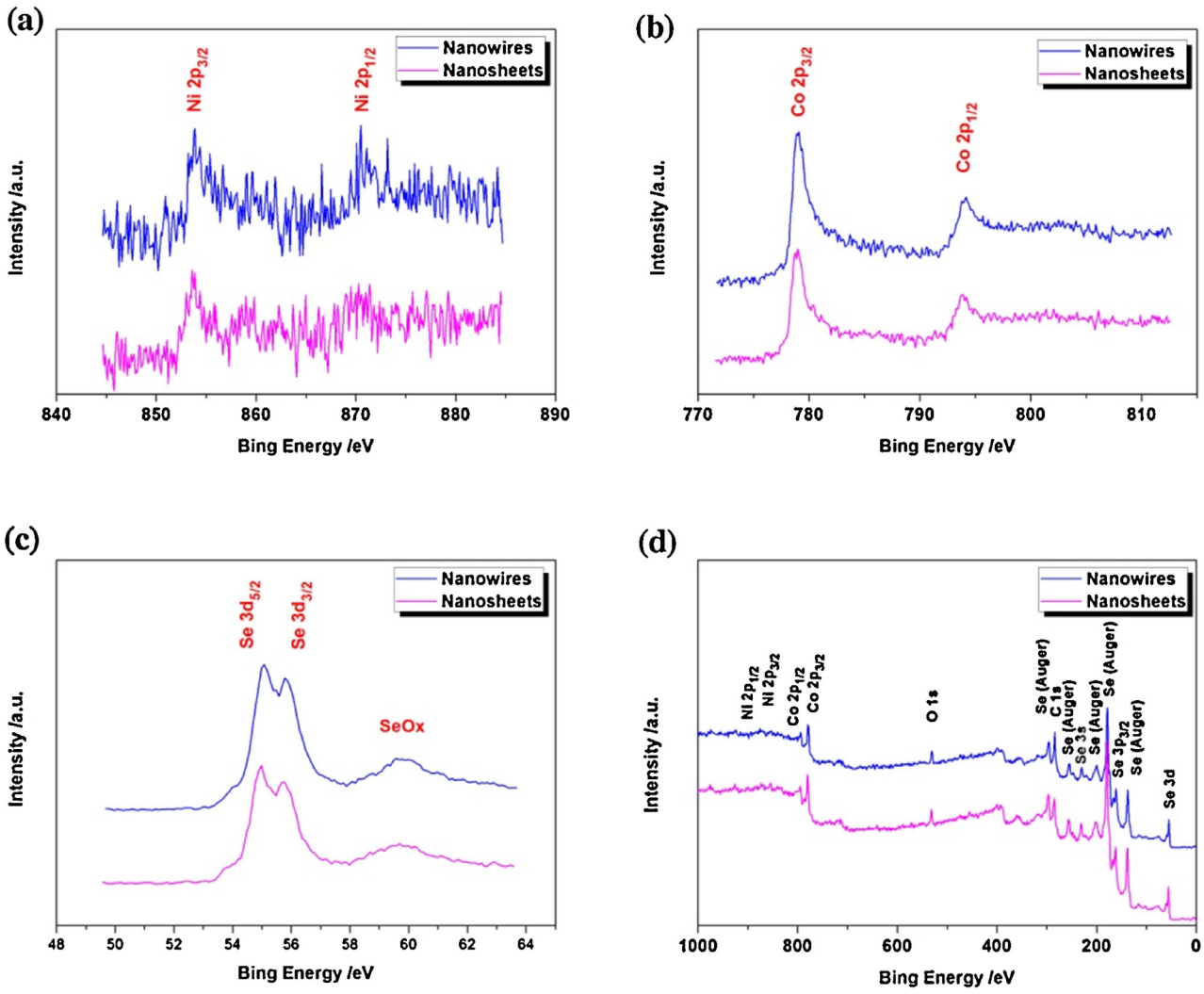

Fig. 7. XPS spectra of $Ni_{1/3}Co_{2/3}Se_2$ nanowires (blue line) and nanosheets (pink line): high resolution of Ni 2p (a), Co 2p (b), Se 3d (c) and survey spectra (d).

(EIS) tests are carried out within the frequency ranging from 100 kHz to 0.1 kHz with an amplitude of 10 mV to investigate the facile kinetics process toward hydrogen evolution. The Nyqusit plots and data fitting to a simplified Randles circuit are supplied in Fig. 8e. $Ni_{1/3}Co_{2/3}Se_2$ nanowires and nanosheets electrodes exhibit small charge-transfer resistance (Rct) of approximate 2.2 Ω and 2.8 Ω, respectively. In addition, the low series resistance (about 2.7 Ω) is observed for both $Ni_{1/3}Co_{2/3}Se_2$ nanowires and nanosheets electrodes. It is believed that the larger accessible surface area ensured by the hierarchically 3D networked nanowire arrays and high intrinsic conductivity by directly growing $Ni_{1/3}Co_{2/3}Se_2$ nanowires on carbon cloth mainly contribute to the better electrochemical HER performance. The excellent HER activity and durability for $Ni_{1/3}Co_{2/3}Se_2$ nanowires and nanosheets is mainly due to the following factors: (1) The unique nanowire arrays and nanosheets with network structure not only provide large surface area allowing for exposure of more active sites, but also facilitates efficient pathways for electrolyte and H_2 evolution. As shown in Fig. 8f, the particular 3D structures provide deep electrolyte penetration for electrons and electrolyte ions during the hydrogen evolution process. (2) The nanowire and nanosheet arrays grow directly on conductive CC substrate to form integrated electrode, which is regarded as beneficial to improve the electric connection between the catalytic material and current collector. (3) Another key advantage of the as-prepared flexible electrodes is the good mechanical adhesion, which can accommodate structural strains and favor an enhanced durability. (4) The direct contact of active materials with conductive substrate can ensure good mechanical adhesion, avoiding the use of polymer binders that generally increase the series resistance and blocking of active sites [23,44].

3. Conclusion

In summary, $Ni_{1/3}Co_{2/3}Se_2$ nanowires and nanosheets have been fabricated on carbon cloth through a facile two-step approach including the first hydrothermal preparation of corresponding $NiCo_2O_4$ nanowires and electrodeposition of $NiCo_2O_4$ nanosheets, accompanied by selenization treatment via simple hydrothermal process. Particularly, the final $Ni_{1/3}Co_{2/3}Se_2$ nanowires are composed of enormous thin nanosheets, which interconnect with each other to form a hierarchically three-dimensional-networked

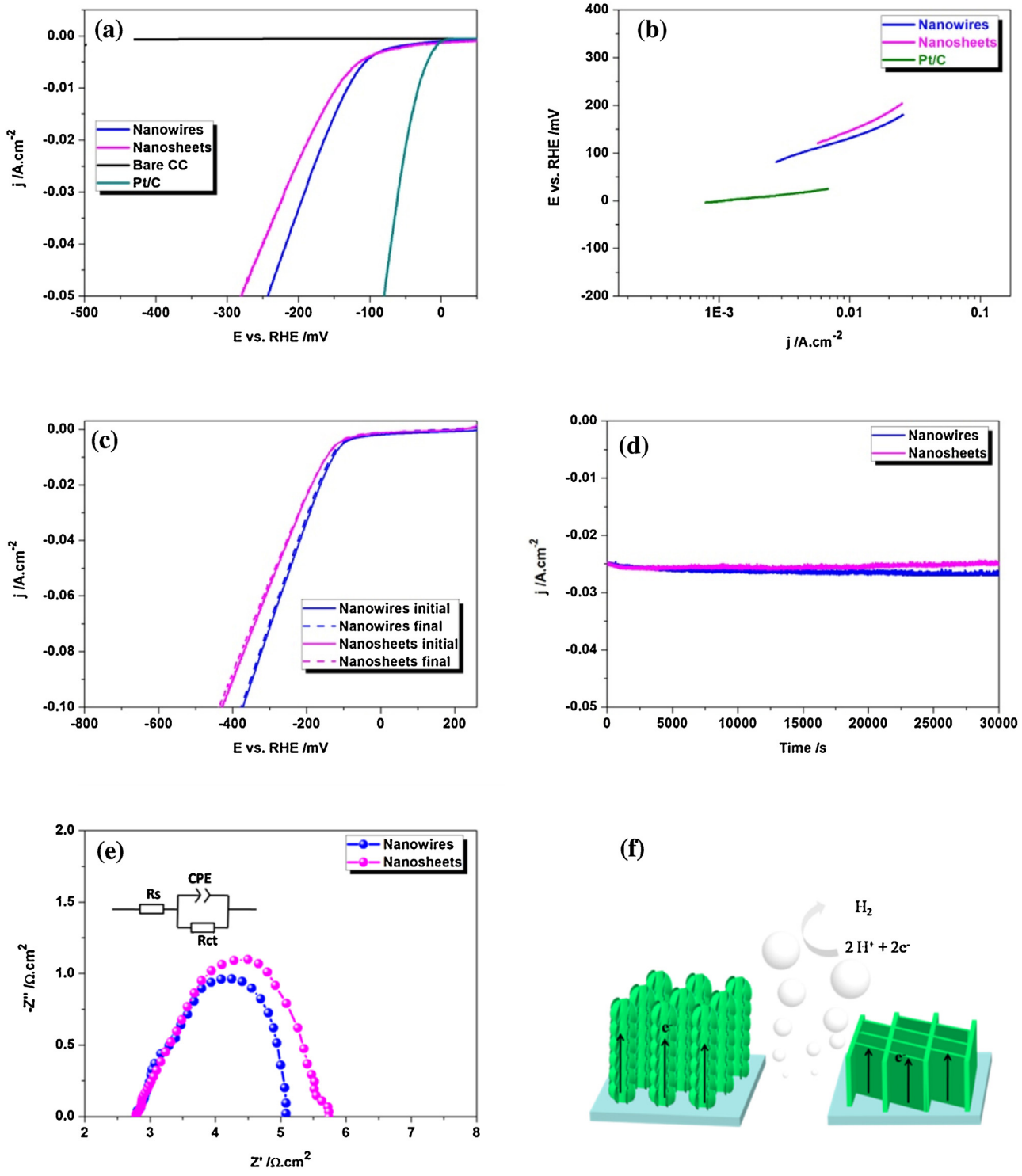

Fig. 8. (a) Polarization curves of $Ni_{1/3}Co_{2/3}Se_2$ nanowires and nanosheets, along with bare CC and 20% wt Pt/C. (b) Tafel plots for $Ni_{1/3}Co_{2/3}Se_2$ nanowires, nanosheets and 20% wt Pt/C. (c) Stability tests of $Ni_{1/3}Co_{2/3}Se_2$ nanowires and nanosheets catalyst through potential cycling, in which the polarization curves before and after 1000 potential cycles are displayed. (d) Time dependent current density curves for $Ni_{1/3}Co_{2/3}Se_2$ nanowires and nanosheets at fixed overpotential in 0.5 M H_2SO_4. (e) Nyqusit plots for the HER of $Ni_{1/3}Co_{2/3}Se_2$ nanowires and nanosheets (Inset is the simplified Randles equivalent circuit). (f) Schematic illustration for the HER process of $Ni_{1/3}Co_{2/3}Se_2$ nanowires and nanosheets.

structure. Such 3D flexible electrodes anchored by nickel cobalt ternary diselenides can be directly used as binder-free electrode for electrochemical hydrogen evolution reaction. The final products show high electrochemical HER activity, excellent durability after potential sweep tests for 1000 cycles and catalytic stability for electrolysis over 8 h. The $Ni_{1/3}Co_{2/3}Se_2$ nanowires and nanosheets electrodes have been proved be advanced catalyst for the HER application.

Acknowledgments

This work was supported by the Grants from National Natural Science Foundation of China (Nos. 11204262), Hunan Provincial Innovation Foundation for Postgraduate (No. CX2014A011), Open Fund based on innovation platform of Hunan colleges and universities (No. 13K045 and 15K128), Key laboratory of optoelectronic Devices and Systems of Ministry of Education and Guangdong Province Fund (No. GD201404).

Appendix A. Supplementary data

Supplementary data associated with this article can be found, in the online version, at http://dx.doi.org/10.1016/j.electacta.2016.03.186.

References

[1] X. Wang, K. Maeda, A. Thomas, K. Takanabe, G. Xin, J.M. Carlsson, K. Domen, M. Antonietti, A metal-free polymeric photocatalyst for hydrogen production from water under visible light, Nature materials 8 (2009) 76–80.
[2] Z. Zeng, C. Tan, X. Huang, S. Bao, H. Zhang, Growth of noble metal nanoparticles on single-layer TiS 2 and TaS 2 nanosheets for hydrogen evolution reaction, Energy & Environmental Science 7 (2014) 797–803.
[3] S. Chen, J. Duan, Y. Tang, B. Jin, S.Z. Qiao, Molybdenum sulfide clusters-nitrogen-doped graphene hybrid hydrogel film as an efficient three-dimensional hydrogen evolution electrocatalyst, Nano Energy 11 (2015) 11–18.
[4] C. Ouyang, X. Wang, S. Wang, Phosphorus-doped CoS 2 nanosheet arrays as ultra-efficient electrocatalysts for the hydrogen evolution reaction, Chemical Communications 51 (2015) 14160–14163.
[5] V. Bansal, A.P. O'Mullane, S.K. Bhargava, Galvanic replacement mediated synthesis of hollow Pt nanocatalysts: Significance of residual Ag for the H 2 evolution reaction, Electrochemistry Communications 11 (2009) 1639–1642.
[6] J.B. Raoof, R. Ojani, S.A. Esfeden, S.R. Nadimi, Fabrication of bimetallic Cu/Pt nanoparticles modified glassy carbon electrode and its catalytic activity toward hydrogen evolution reaction, International Journal of Hydrogen Energy 35 (2010) 3937–3944.
[7] X. Cao, Y. Han, C. Gao, Y. Xu, X. Huang, M. Willander, N. Wang, Highly catalytic active PtNiCu nanochains for hydrogen evolution reaction, Nano Energy 9 (2014) 301–308.
[8] W.-F. Chen, C.-H. Wang, K. Sasaki, N. Marinkovic, W. Xu, J. Muckerman, Y. Zhu, R. Adzic, Highly active and durable nanostructured molybdenum carbide electrocatalysts for hydrogen production, Energy & Environmental Science 6 (2013) 943–951.
[9] X. Zheng, J. Xu, K. Yan, H. Wang, Z. Wang, S. Yang, Space-confined growth of MoS2 nanosheets within graphite: The layered hybrid of MoS2 and graphene as an active catalyst for hydrogen evolution reaction, Chemistry of Materials 26 (2014) 2344–2353.
[10] M.A. Lukowski, A.S. Daniel, C.R. English, F. Meng, A. Forticaux, R.J. Hamers, S. Jin, Highly active hydrogen evolution catalysis from metallic WS 2 nanosheets, Energy & Environmental Science 7 (2014) 2608–2613.
[11] M.A. Lukowski, A.S. Daniel, C.R. English, F. Meng, A. Forticaux, R.J. Hamers, S. Jin, Highly active hydrogen evolution catalysis from metallic WS2nanosheets, Energy & Environmental Science 7 (2014) 2608.
[12] F.H. Saadi, A.I. Carim, J.M. Velazquez, J.H. Baricuatro, C.C.L. McCrory, M.P. Soriaga, N.S. Lewis, OperandoSynthesis of Macroporous Molybdenum Diselenide Films for Electrocatalysis of the Hydrogen-Evolution Reaction, ACS Catalysis 4 (2014) 2866–2873.
[13] H. Wang, D. Kong, P. Johanes, J.J. Cha, G. Zheng, K. Yan, N. Liu, Y. Cui, MoSe2 and WSe2 nanofilms with vertically aligned molecular layers on curved and rough surfaces, Nano letters 13 (2013) 3426–3433.
[14] C. Ge, P. Jiang, W. Cui, Z. Pu, Z. Xing, A.M. Asiri, A.Y. Obaid, X. Sun, J. Tian, Shape-controllable synthesis of Mo 2C nanostructures as hydrogen evolution reaction electrocatalysts with high activity, Electrochimica Acta 134 (2014) 182–186.
[15] D.V. Esposito, S.T. Hunt, A.L. Stottlemyer, K.D. Dobson, B.E. McCandless, R.W. Birkmire, J.G. Chen, Low-Cost Hydrogen-Evolution Catalysts Based on Monolayer Platinum on Tungsten Monocarbide Substrates, Angewandte Chemie International Edition 49 (2010) 9859–9862.
[16] E.J. Popczun, J.R. McKone, C.G. Read, A.J. Biacchi, A.M. Wiltrout, N.S. Lewis, R.E. Schaak, Nanostructured nickel phosphide as an electrocatalyst for the hydrogen evolution reaction, Journal of the American Chemical Society 135 (2013) 9267–9270.
[17] J.F. Callejas, C.G. Read, E.J. Popczun, J.M. McEnaney, R.E. Schaak, Nanostructured Co2P Electrocatalyst for the Hydrogen Evolution Reaction and Direct Comparison with Morphologically Equivalent CoP, Chemistry of Materials 27 (2015) 3769–3774.
[18] J.M. McEnaney, J.C. Crompton, J.F. Callejas, E.J. Popczun, A.J. Biacchi, N.S. Lewis, R.E. Schaak, Amorphous molybdenum phosphide nanoparticles for electrocatalytic hydrogen evolution, Chemistry of Materials 26 (2014) 4826–4831.
[19] H. Vrubel, X. Hu, Molybdenum boride and carbide catalyze hydrogen evolution in both acidic and basic solutions, Angewandte Chemie 124 (2012) 12875–12878.
[20] P. Zheng, J. Zhao, J. Zheng, G. Ma, Z. Zhu, Non-equilibrium partial oxidation of TiN surface for efficient visible-light-driven hydrogen production, Journal of Materials Chemistry 22 (2012) 12116–12120.
[21] H. Zhou, Y. Wang, R. He, F. Yu, J. Sun, F. Wang, Y. Lan, Z. Ren, S. Chen, One-step synthesis of self-supported porous NiSe 2/Ni hybrid foam: An efficient 3D electrode for hydrogen evolution reaction, Nano Energy 20 (2016) 29–36.
[22] C. Ouyang, X. Wang, C. Wang, X. Zhang, J. Wu, Z. Ma, S. Dou, S. Wang, Hierarchically Porous Ni 3 S 2 Nanorod Array Foam as Highly Efficient Electrocatalyst for Hydrogen Evolution Reaction and Oxygen Evolution Reaction, Electrochimica Acta 174 (2015) 297–301.
[23] Q. Liu, J. Shi, J. Hu, A.M. Asiri, Y. Luo, X. Sun, CoSe2Nanowires Array as a 3D Electrode for Highly Efficient Electrochemical Hydrogen Evolution, ACS applied materials & interfaces 7 (2015) 3877–3881.
[24] M.-R. Gao, Z.-Y. Lin, T.-T. Zhuang, J. Jiang, Y.-F. Xu, Y.-R. Zheng, S.-H. Yu, Mixed-solution synthesis of sea urchin-like NiSe nanofiber assemblies as economical Pt-free catalysts for electrochemical H 2 production, Journal of Materials Chemistry 22 (2012) 13662–13668.
[25] W. Cui, C. Ge, Z. Xing, A.M. Asiri, X. Sun, Ni x S y-MoS 2 hybrid microspheres: One-pot hydrothermal synthesis and their application as a novel hydrogen evolution reaction electrocatalyst with enhanced activity, Electrochimica Acta 137 (2014) 504–510.
[26] M.-R. Gao, Y.-F. Xu, J. Jiang, Y.-R. Zheng, S.-H. Yu, Water oxidation electrocatalyzed by an efficient Mn3O4/CoSe2 nanocomposite, Journal of the American Chemical Society 134 (2012) 2930–2933.
[27] M.-R. Gao, W.-T. Yao, H.-B. Yao, S.-H. Yu, Synthesis of Unique Ultrathin Lamellar Mesostructured CoSe2- Amine (Protonated) Nanobelts in a Binary Solution, Journal of the American Chemical Society 131 (2009) 7486–7487.
[28] M.R. Gao, Q. Gao, J. Jiang, C.H. Cui, W.T. Yao, S.H. Yu, A Methanol-Tolerant Pt/CoSe2 Nanobelt Cathode Catalyst for Direct Methanol Fuel Cells, Angewandte Chemie 123 (2011) 5007–5010.
[29] M. Gao, J. Liang, Y. Zheng, Y. Xu, J. Jiang, Q. Gao, J. Li, S. Yu, An efficient molybdenum disulfide/cobalt diselenide hybrid catalyst for electrochemical hydrogen generation, Nature communications 6 (2014) 5982-5982.
[30] Y.F. Xu, M.R. Gao, Y.R. Zheng, J. Jiang, S.H. Yu, Nickel/nickel (II) oxide nanoparticles anchored onto cobalt (IV) diselenide nanobelts for the electrochemical production of hydrogen, Angewandte Chemie International Edition 52 (2013) 8546–8550.
[31] D. Kong, J.J. Cha, H. Wang, H.R. Lee, Y. Cui, First-row transition metal dichalcogenide catalysts for hydrogen evolution reaction, Energy & Environmental Science 6 (2013) 3553–3558.
[32] H. Zhang, B. Yang, X. Wu, Z. Li, L. Lei, X. Zhang, Polymorphic CoSe2with Mixed Orthorhombic and Cubic Phases for Highly Efficient Hydrogen Evolution Reaction, ACS applied materials & interfaces 7 (2015) 1772–1779.
[33] K. Wang, D. Xi, C. Zhou, Z. Shi, H. Xia, G. Liu, G. Qiao, CoSe 2 necklace-like nanowires supported by carbon fiber paper: a 3D integrated electrode for the hydrogen evolution reaction, Journal of Materials Chemistry A 3 (2015) 9415–9420.
[34] Y.-R. Zheng, M.-R. Gao, Z.-Y. Yu, Q. Gao, H.-L. Gao, S.-H. Yu, Cobalt diselenide nanobelts grafted on carbon fiber felt: an efficient and robust 3D cathode for hydrogen production, Chemical Science 6 (2015) 4594–4598.
[35] R. Ding, L. Qi, M. Jia, H. Wang, Facile synthesis of mesoporous spinel NiCo 2 O 4 nanostructures as highly efficient electrocatalysts for urea electro-oxidation, Nanoscale 6 (2014) 1369–1376.
[36] D. Guo, Y. Luo, X. Yu, Q. Li, T. Wang, High performance NiMoO4 nanowires supported on carbon cloth as advanced electrodes for symmetric supercapacitors, Nano Energy 8 (2014) 174–182.
[37] B. Yuan, W. Luan, S.-t. Tu, One-step solvothermal synthesis of nickel selenide series: Composition and morphology control, CrystEngComm 14 (2012) 2145–2151.
[38] Y.R. Zheng, M.R. Gao, Q. Gao, H.H. Li, J. Xu, Z.Y. Wu, S.H. Yu, An Efficient CeO2/CoSe2 Nanobelt Composite for Electrochemical Water Oxidation, Small 11 (2015) 182–188.
[39] M. Basu, Z.-W. Zhang, C.-J. Chen, P.-T. Chen, K.-C. Yang, C.-G. Ma, C.C. Lin, S.-F. Hu, R.-S. Liu, Heterostructure of Si and CoSe2: A Promising Photocathode Based on a Non-noble Metal Catalyst for Photoelectrochemical Hydrogen Evolution, Angewandte Chemie International Edition 54 (2015) 6211–6216.
[40] J. Yang, G.-H. Cheng, J.-H. Zeng, S.-H. Yu, X.-M. Liu, Y.-T. Qian, Shape control and characterization of transition metal diselenides MSe2 (M = Ni, Co Fe) prepared by a solvothermal-reduction process, Chemistry of Materials 13 (2001) 848–853.

[41] C. de las Heras, F. Agulló-Rueda, Raman spectroscopy of NiSe2 and NiS2-xSex (0< x< 2) thin films, Journal of Physics Condensed Matter 12 (2000) 5317–5324.
[42] W. Wei, L. Mi, Y. Gao, Z. Zheng, W. Chen, X. Guan, Partial Ion-Exchange of Nickel-Sulfide-Derived Electrodes for High Performance Supercapacitors, Chemistry of Materials 26 (2014) 3418–3426.
[43] D. Kong, H. Wang, Z. Lu, Y. Cui, CoSe2Nanoparticles Grown on Carbon Fiber Paper: An Efficient and Stable Electrocatalyst for Hydrogen Evolution Reaction, Journal of the American Chemical Society 136 (2014) 4897–4900.
[44] K. Xu, F. Wang, Z. Wang, X. Zhan, Q. Wang, Z. Cheng, M. Safdar, J. He, Component-Controllable WS2 (1–x) Se2 x Nanotubes for Efficient Hydrogen Evolution Reaction, ACS nano 8 (2014) 8468–8476.